DOI: 10.1002/ejic.201000168

Actinyl Compounds with Hexavalent Elements (S, Cr, Se, Mo) – Structural Diversity, Nanoscale Chemistry, and Cellular Automata Modeling

Sergey V. Krivovichev*[a]

Keywords: Actinides / Uranium / Crystal structure / Nanotubes / Cellular automata

Actinyl oxysalts with TO_4 tetrahedral oxyanions (T = S, Se, Cr, Mo) demonstrate a remarkable structural diversity, owing to the flexibility of the An–O–T linkages, which results in a multitude of topological and geometrical variations. Application of graph representation of structural units allows topological classification of structures and analysis of topological and geometrical isomers. In some organically templated structures, isomerism is controlled by the interplay of hydrophobic/hydrophilic interactions between organic and inorganic substructures. The high flexibility of actinyl oxysalt complexes (in particular, in uranyl selenates) allows strong curvature of inorganic units and formation of curved nanoscale tubules assembled from [1+4+1] complexes. In some particular systems, the self-assembly process may be modeled using a cellular automata approach.

1. Introduction

Actinide and, especially, uranium oxysalts with hexavalent cations of the elements of the sixth group of the periodic table are important phases from the mineralogical, environmental, and technological points of view. These compounds are common constituents of the oxidized zones of uranium mineral deposits,[1] form as a result of the alteration of spent nuclear fuel (SNF),[2] form during burn-up of nuclear fuels in reactors,[3] represent insoluble residues undesirable for the recovery of plutonium from SNF solutions,[4] impact upon the transport of actinides in contaminated soils,[5] and upon the mobility of radionuclides in a geological repository for nuclear waste,[6] etc. In addition, they are of interest from the viewpoint of physical properties such as luminescence and magnetism induced by the f electrons in the electronic structure of actinide ions. From the fundamental viewpoint, these compounds are remarkable in their wide range of compositions and structures originating from combinatorial and topological possibilities of linkage of basic structural elements that leads to a large variety of topological and geometrical isomers. A review of the whole range of structures that occur in actinide oxysalts with the elements of the sixth group of the periodic table was published elsewhere;[7] some recent results are summarized in ref.[8] In this microreview, we outline the basic structural features of one particular group of these compounds, namely those in which actinyl ions are polymerized through tetrahedral oxyanions TO_4 (T = S, Cr, Se, and Mo). We also concentrate on the origin of structural diversity from the algorithmic viewpoint that links descriptive chemistry to the theories of graphs and cellular automata. Application of the concepts of these abstract mathematical theories to the description of chemical and structural variations may provide further insight into algorithms of self-assembly in real chemical systems.

[a] Department of Crystallography, St. Petersburg State University, University Emb. 7/9, 199034 St. Petersburg, Russia
Fax: +7-812-3506688
E-mail: skrivovi@mail.ru

2. Topology of Structural Polymerization: Basic Graph, Its Variations, and Topological Isomerism

In their high oxidation states, actinide ions usually form linear actinyl complexes $[O=An^{n+}=O]^{(n-4)+}$ in which the valence requirements of terminal O atoms are more or less satisfied (Figure 1). As a result, linkage of actinyl ions to

Sergey V. Krivovichev received his Ph.D. (1997) and D.Sc. (2002) degrees from St. Petersburg State University. During 1999–2005, he held a number of fellowships that allowed him to perform collaborative research in structural chemistry, mineralogy, and crystallography in the U.S.A. (University of Notre Dame), Germany (University of Kiel), and Austria (University of Innsbruck). From 2005 until the present he is a Full Professor and Chairman of the Department of Crystallography at St. Petersburg State University. He has co-authored over 200 scientific papers and 6 books. In 2002, he has been awarded the Medal for Research Excellence by the European Mineralogical Union. In 2008, he received the President of the Russian Federation Award in Science and Technology for Young Scientists.

other structural elements proceeds along bonding to actinyl ions in their equatorial planes. In actinyl sulfates, molybdates, selenates, and chromates, actinyl ions are equatorially coordinated by O atoms of tetrahedral complexes or OH groups and H_2O molecules. The most frequently observed coordination is fivefold, leading to the formation of a flattened pentagonal bipyramid, AnO_7, centered by an actinide ion (Figure 1b). Usually, coordination of an actinyl ion by a TO_4 tetrahedron is monodentate (AnO_7 and TO_4 groups share one O atom only), though bidentate coordination is quite common in uranyl sulfates.[9] Polymerization of actinyl ions through tetrahedral oxyanions results in formation of a whole family of extended complexes with different compositions and topologies (Figure 1c). The general formula of such complexes may be written as $[(AnO_2)_p(TO_4)_q(H_2O)_r]$. Two examples of 2D layers with the same composition $[(UO_2)_2(SeO_4)_3(H_2O)]^{2-}$ are shown in Figure 2a, b. The topology of the complexes is very similar, but still one cannot be transformed into another by continuous topological transformation, that is, without breaking of chemical bonds. The easiest way to identify topological differences between two layers is to draw their graphs. The graph can be constructed by elimination of anions from consideration and linking those U and Se atoms that share at least one common O atom (Figure 2c, d). As it can be seen, the graphs shown in Figure 2c and d are composed from the same relative numbers of four- and six-membered rings (MRs). We identify these topologies as **1** and **2**, respectively (Table 1). Description of complexes in terms of graphs demonstrates clearly that, in topology **1**, six-membered rings form edge-sharing chains, whereas, in topology **2**, they form corner-sharing chains. Therefore, these topologies should be regarded as different, and their corresponding uranyl selenate complexes should be considered as *topological* isomers.

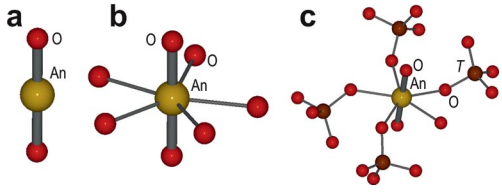

Figure 1. Linear actinyl ion $[O=An^{n+}=O]^{(n-4)+}$ (a) and its coordination by equatorial anions (b) and tetrahedral oxyanions (c).

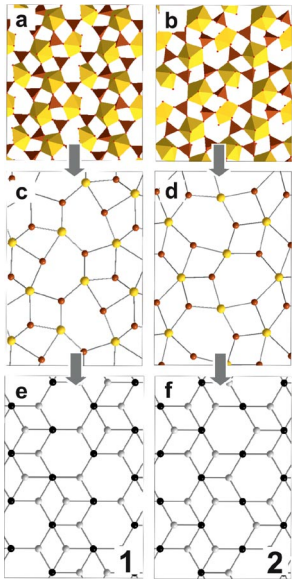

Figure 2. Uranyl selenate layers $[(UO_2)_2(SeO_4)_3(H_2O)]^{2-}$ with different topologies of linkage of U (yellow) and Se (brown) coordination polyhedra (a, b): presentation as graphs (c, d) and as idealized graphs (e, f).

Table 1. Actinyl compounds with topologies characterized by graphs shown in Figure 3 (examples).

Topology	Compound	Reference
1	$[N_2C_3H_{12}][(UO_2)_2(H_2O)(SO_4)_3]$	[22f]
	$[C_4H_{12}N]_2[(UO_2)_2(SeO_4)_3(H_2O)]$	[16]
2	$[N_2C_3H_{12}][(NpO_2)_2(CrO_4)_3(H_2O)](H_2O)_3$	[11a]
	$K_2[(NpO_2)_2(CrO_4)_3(H_2O)](H_2O)_3$	[11b]
	$[C_8H_{22}N_2][(UO_2)_2(SeO_4)_3(H_2O)]$	[16]
4	$[C_8H_{26}N_4]_{0.5}[(UO_2)_2(SO_4)_3(H_2O)]$	[11c]
5	$Rb_2[(UO_2)_2(SeO_4)_3(H_2O)_2](H_2O)_4$	[11d]
6	$K_2[(UO_2)_2(CrO_4)_3(H_2O)_2](H_2O)_4$	[11e]
7	$Mg_2[(UO_2)_3(CrO_4)_5](H_2O)_{17}$	[15]
	β-$Mg_2[(UO_2)_3(SeO_4)_5](H_2O)_{16}$	[11f]
8	$(NH_3(CH_2)_3NH_3)(H_3O)_2[(UO_2)_3(MoO_4)_5]$	[23a]
	$Na_6[(Np^{5+}O_2)_2(Np^{6+}O_2)(MoO_4)_5](H_2O)_{13}$	[11g]
	α-$Mg_2[(UO_2)_3(SeO_4)_5](H_2O)_{16}$	[11f]

We note that graphs shown in Figure 2c and d can be topologically transformed into graphs shown in Figure 2e and f, respectively. In turn, the latter two graphs are derivatives of the ideal graph **3** shown in Figure 3. This graph consists of 6-connected black and 4-connected white vertices and was identified as the basic graph, as it is a parent graph to several dozens of topologies observed in the structures of inorganic oxysalts.[10] Figure 3 shows some examples of the topological derivatives, and Table 1 provides a list of the corresponding actinyl compounds. These exam-

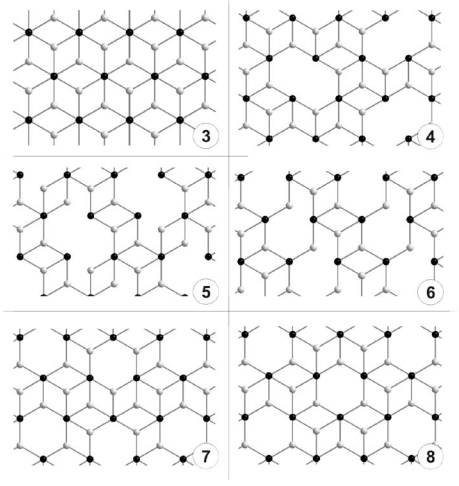

Figure 3. Basic graph (**3**) and its derivative graphs that appear as underlying topologies for actinyl oxysalts with tetrahedral oxyanions TO_4 (T = S, Cr, Se, and Mo) (see Table 1 for the example compounds).

ples show that topological isomerism is a common phenomenon for actinyl complexes occurring in the structures of sulfates, chromates, molybdates, and selenates.

3. Geometrical Isomerism

The topological structure of a heteropolyhedral complex observed in actinyl oxysalts cannot be completely characterized by its graph. Figure 4 shows three 1D chains with identical formula, $[AnO_2(TO_4)(H_2O)_2]$, and identical graphs. Within the chains, the $AnO_5(H_2O)_2$ pentagonal bipyramids share three equatorial O atoms with TO_4 tetrahedra, whereas TO_4 tetrahedra have three vertices each shared with actinyl pentagonal bipyramids and one apical ligand that points either up (u) or down (d) relative to the plane of the chain. In different structures, the orientations of apical ligands along the chain extension may be different. For example, in the structures of $[UO_2(CrO_4)(H_2O)_2]$ and $[UO_2(CrO_4)(H_2O)_2](H_2O)$,[12] the orientations alternate in the order "...up-down-up-down..." or ...udud... [or $(ud)_\infty$] (Figure 4b). In contrast, the structure of $[UO_2(CrO_4)(H_2O)_2]_4(H_2O)_9$[13] contains two types of chains: one with the sequence ...ududud... [= $(ud)_\infty$] and one with the sequence ...uuuu... [= $(u)_\infty$] with the nonshared corners of chromate tetrahedra on one side of the chain only (Figure 4a). The structure of β-$[UO_2(SO_4)(H_2O)_2](H_2O)_3$[14] contains chains with the sequence ...uudduudd... or $(uudd)_\infty$. We note that, despite different orientations of tetrahedra, the three chains shown in Figure 4 correspond to the same graph. The three chains should be considered as geometrical isomers, that is, chemical structures have the same global topology (e.g., graph) but are different because of some specific properties of linkage (e.g., *cis*-*trans*-isomerism). It is likely that, in actinyl oxysalts, the occurrence of a certain type of isomer is impacted by the specificity of interactions of polyhedral units with each other and with other structural elements. In the case of uranyl chromate hydrates mentioned above, it seems that the occurrence of isomers is related to the number of water molecules present in the structure, that is, by features of the hydrogen-bonding system.

In the case of 2D layers, arrangement of orientations of tetrahedral oxyanions relative to the layer plane can be quite complex. Figure 5 shows three 2D graphs that represent topology **7** (Figure 3) of linkage of uranyl pentagonal bipyramids and chromate tetrahedra in structures of uranyl chromates with $[(UO_2)_3(CrO_4)_5]^{4-}$ anionic layers.[15] Symbols u and d written near the white vertices indicate the orientations of chromate tetrahedra: up or down. Transferring the lattice of these symbols onto a 2D plane and using the symbol "□" to denote vacancy (absence of white vertex in the specific position of the graph), one may obtain a 2D square array of symbols that can be characterized by its "unit cell" confined in orthogonal boxes in Figure 5d, e, and f. This "unit cell" or matrix of orientations of tetrahedra is a unique descriptor of a particular geometrical isomer.

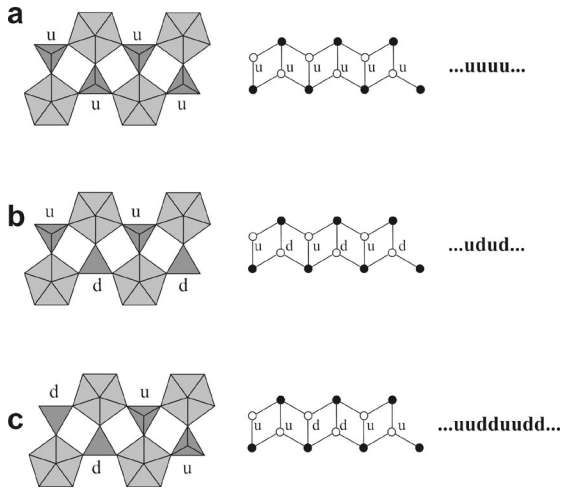

Figure 4. The description of geometrical isomerism of the $[AnO_2(TO_4)(H_2O)_2]$ chains.

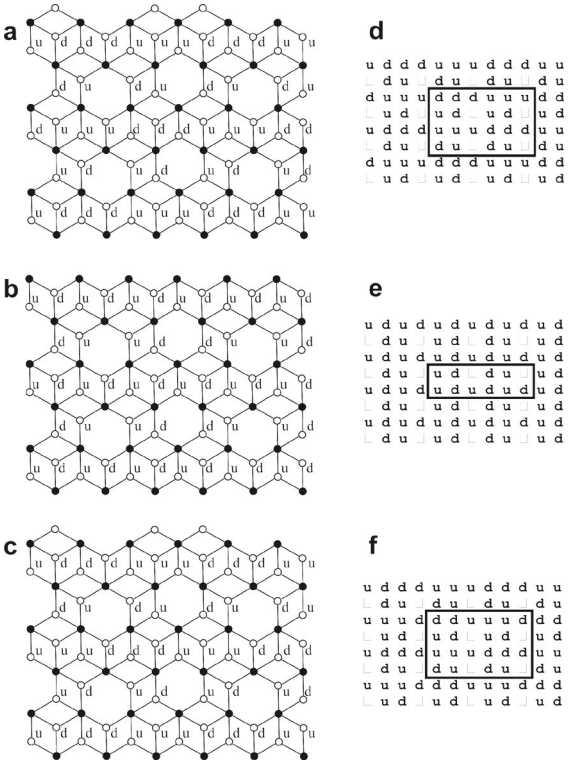

Figure 5. Black-and-white graphs with the u, d, and □ symbols of the $[(UO_2)_3(CrO_4)_5]$ sheets in the structures of $Mg_2[(UO_2)_3(CrO_4)_5](H_2O)_{17}$ (a), $Ca_2[(UO_2)_3(CrO_4)_5](H_2O)_{19}$ (b), and $K_4[(UO_2)_3(CrO_4)_5](H_2O)_8$ (c); their corresponding u, d, and □ symbolic tables [(d), (e), and (f), respectively]. The matrices of orientation of tetrahedra are indicated in (d), (e), and (f) by bold lines.

It should be noted that the system of orientation of tetrahedra in different geometrical isomers may be chiral, which can be clearly identified by analysis of their matrix descriptors. For instance, topology **1**, observed in uranyl selenates and sulfates, has two geometrical isomers observed so far, one of them being chiral (the corresponding compounds crystallize in the chiral space group $P2_1$).[16]

4. Uranyl Selenate Nanotubules: Geometry and Packing Principles

Along with actinide peroxide nanospheres[17] and plutonium colloids,[18] uranyl selenate nanotubules are one of the few known purely inorganic nanoscale actinide structures (though several metal–organic tubular and cluster structures have recently been reported[19]). The tubules represent one-dimensional porous structures formed by linking uranyl pentagonal bipyramids to SeO_4 tetrahedra through common O atoms. There are two types of nanotubules reported so far. "Small" tubules (Figure 6) have been found in two structures.[20a,20c] Their composition is characterized by their U/Se ratio, which is equal to 3:5, so the chemical formula is $[(UO_2)_3(SeO_4)_5]^{4-}$, and the structure is stabilized by the presence of positively charged species, namely, K^+ cations. The local topology of the tubules is isomorphous to topology **8** shown in Figure 3. This topology displays a tendency to form geometrical isomers with different systems of orientations of tetrahedra relative to the plane of the sheets. For 2D topologies, the ratio u/d of "up" and "down" orientations is invariably 1:1. However, the situation is different for uranyl selenate nanotubules, where the u/d ratio is equal to 4:1 (defining "up" orientation as pointing out of the tubules and "down" orientation as pointing inside the tubule). Thus, whereas for 2D structures, there is no difference between orientations of tetrahedra (two half-spaces separated by the sheet are chemically indistinguishable), for cylindrical (tubular) topologies, the space is separated into exterior and interior, which are both geometrically and chemically different.

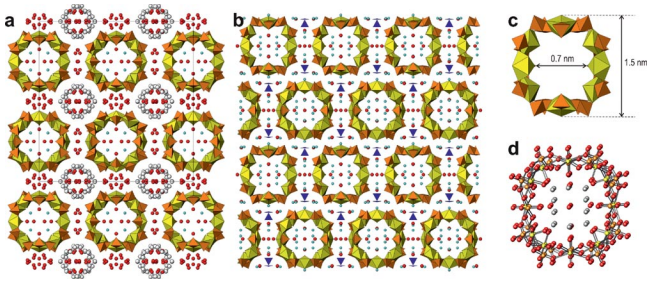

Figure 6. Crystal structures of $K_5[(UO_2)_3(SeO_4)_5](NO_3)(H_2O)_{3.5}$ (a) and $(H_3O)_2K[(H_3O)@(18\text{-crown-6})][(UO_2)_3(SeO_4)_5](H_2O)_4$ (b) containing "small" uranyl selenate nanotubules with a U/Se ratio of 3:5 (c, d). Uranyl and selenium coordination polyhedra are shown as yellow and light-brown, respectively.

The geometry of the 3:5 uranyl selenate nanotubules is almost identical in the two structures reported so far. The parameter along the tubule is equal to 11.293 Å in $K_5[(UO_2)_3(SeO_4)_5](NO_3)(H_2O)_{3.5}$ and 11.240 Å in $(H_3O)_2K[(H_3O)@(18\text{-crown-6})][(UO_2)_3(SeO_4)_5](H_2O)_4$. Figure 7 shows a diagram that demonstrates the geometrical similarity of the tubules in the two structures in terms of the U–O–Se valence angles. The dotted line corresponds to the ideal case, when all corresponding angles are equal, whereas the deviation of points from this line shows the difference between the corresponding angles in the two structures. It is clear from the diagram that this difference does not exceed 5–6°, which means that the tubules have very similar geometrical parameters in different structures. Remarkably, the local rod symmetry group of the tubules is the same (*mm*2) and consists of two vertical mutually perpendicular mirror planes intersecting along the twofold symmetry axis.

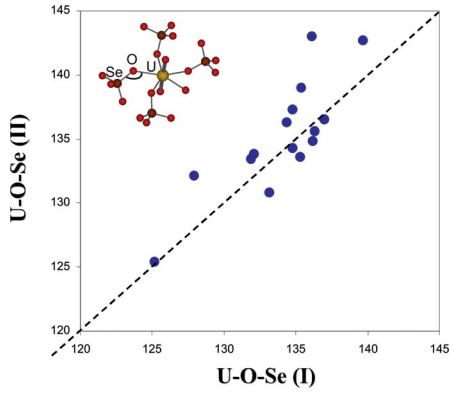

Figure 7. Diagram showing the difference of the U–O–Se valence angle values in uranyl selenate nanotubules in the structures of $K_5[(UO_2)_3(SeO_4)_5](NO_3)(H_2O)_{3.5}$ (**I**) and $(H_3O)_2K[(H_3O)@(18\text{-crown-6})][(UO_2)_3(SeO_4)_5](H_2O)_4$ (**II**).

The observed arrangements of 3:5 uranyl selenate nanotubules are schematically illustrated in Figure 8. They can be rationalized in terms of a sum of axial rotations and vertical shifts of tubules relative to each other. The tubules may be shifted relative to each other by ±1/2 translations along the tubule extension. Thus, there are two different vertical positions of tubules indicated as 0 and 1/2 in Figure 8. The tubules also allow axial positions rotated relative to each other by 90°; these are distinguished in Figure 8 by white and black triangles. The schemes of arrangement of tubules in the two structures are shown in Figure 8c and d. In the structure of $K_5[(UO_2)_3(SeO_4)_5](NO_3)(H_2O)_{3.5}$, the tubules are packed in a hexagonal fashion (the tubules are parallel, and their cross-sections imitate the hexagonal packing of circles), whereas, in $(H_3O)_2K[(H_3O)@(18\text{-crown-6})][(UO_2)_3(SeO_4)_5](H_2O)_4$, the tubules are arranged in a tetragonal packing fashion, which is the result of the presence of single columns of stacked $[(H_3O)@(18\text{-crown-6})]^+$ complexes.

The two structures with 3:5 tubules possess K^+ cations located inside the tubules and showing remarkably similar local coordination to the tube walls (Figure 9). In both structures, K^+ cations are coordinated by six anions of the uranyl selenate wall: two O atoms of the uranyl ions, two nonbridging O atoms of selenate tetrahedra (namely, those oriented toward the *inside* of the tubule), and two O atoms bridging between uranyl ions and selenate tetrahedra. As a whole, the K^+ ion coordinates the [1+4+1] complex that was proposed as a basic unit present in uranyl selenate aqueous solution. It can be hypothesized that hydrated $\{K[(UO_2)_2(SeO_4)_4]\}$ units play the role of precrystallization building units from which the tubules assemble during the crystallization process. From the structural viewpoint, it is beyond any doubt that it is the K^+ ion that is responsible for the formation of curved topologies in 3:5 uranyl selenate

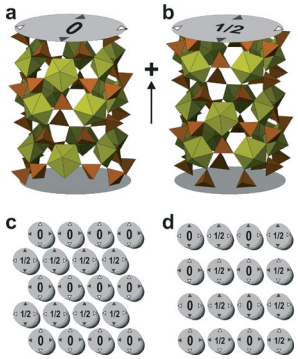

Figure 8. Two orientations of uranyl selenate nanotubules rotated relative to each other by 90° and shifted by 1/2 translation along the axis of a tubule (a, b) and schemes of arrangements of nanotubules in the structures of $K_5[(UO_2)_3(SeO_4)_5](NO_3)(H_2O)_{3.5}$ (c) and $(H_3O)_2K[(H_3O)@(18\text{-crown-6})][(UO_2)_3(SeO_4)_5](H_2O)_4$ (d).

nanotubules. By forming relatively strong K^+–O bonds to uranyl O atoms, it forces inclination of the adjacent linear uranyl ions towards each other, thus inducing curvature of the usually planar uranyl oxysalt units. The fact that tubules do not form in the presence of other alkali metal cations (Na^+, Rb^+, Cs^+) points out to the perfect geometrical adjustments provided by the size of the K^+ ions.

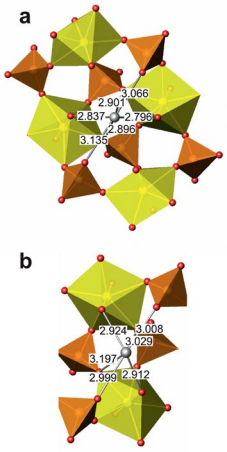

Figure 9. Coordination of K^+ cations relative to the walls of uranyl selenate nanotubules in the structures of $K_5[(UO_2)_3(SeO_4)_5](NO_3)(H_2O)_{3.5}$ (a) and $(H_3O)_2K[(H_3O)@(18\text{-crown-6})][(UO_2)_3(SeO_4)_5](H_2O)_4$ (b).

In addition to "small" 3:5 tubules, uranyl selenates provide another type of tubules with the ratio U/Se of 14:17[20b] and external diameter of approximately 2.5 nm (Figure 10). This tubule does not have isomorphous topology among 2D uranyl selenate sheets known to date. The mechanism of formation of this type of tubules is not clear; however, some possible directions can be outlined.

The tubules are most probably templated by aggregates of protonated butylamine molecules driven by delicate balancing between hydrophilic/hydrophobic interactions. Although the organic substructure in the original 14:17 nanotubular structure was not located, some similarities may be inferred by the analysis of the structure of $(H_3O)_2[C_{12}H_{30}N_2]_3[(UO_2)_4(SeO_4)_8](H_2O)_5$[21] shown in Figure 11. In this structure, protonated 1,12-diaminododecane molecules form cylindrical micelles with amine head groups on the surface that are surrounded by uranyl selenate sheets. The micelle dimensions are approximately elliptical with a cross-section of 2.2×2.5 nm. In order to adapt to the micelles, inorganic sheets possess a strong curvature, the modulations of the adjacent sheets being in antiphase. Taking into account that 1,12-diaminododecane is about twice as long as the butylamine chain, it seems likely that the 14:17 nanotubules owe their formation to micellar aggregates of protonated butylamine molecules.

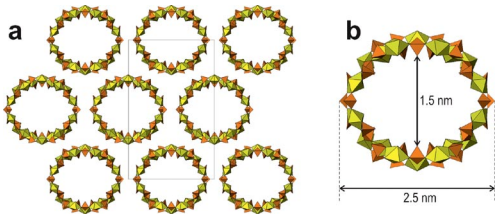

Figure 10. Arrangement of the 14:17 uranyl selenate nanotubules in the structure of $(C_4H_{12}N)_{14}[(UO_2)_{10}(SeO_4)_{17}(H_2O)]$ (a) and cross-section of the nanotubule (b).

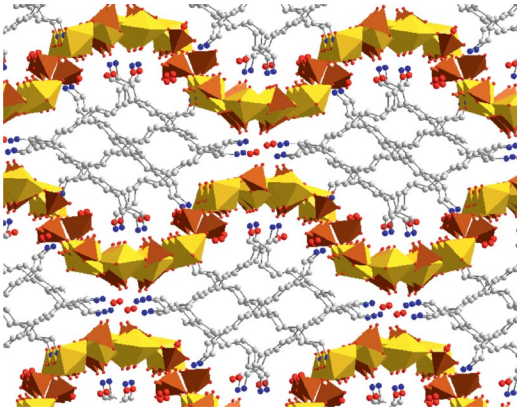

Figure 11. Structure of $(H_3O)_2[C_{12}H_{30}N_2]_3[(UO_2)_4(SeO_4)_8](H_2O)_5$ with modulated uranyl selenate sheets and micellar aggregates of protonated 1,12-diaminododecane molecules (C, N, and H_2O are shown as gray, blue, and red, respectively; H atoms are omitted for clarity).

5. Organically Templated Structures: Molecular Control of Structural Architectures

There are many organically templated uranyl sulfates,[9c,22] molybdates,[23] chromates,[24] and selenates known. However, systematic studies of the influence of template structure upon topology and geometry of inorganic substructure have been (at least partially) performed for uranyl selenates only, because of their relatively simple synthesis conditions and their ability to form crystals of good enough quality for structural characterization.

In particular, interactions of uranyl selenates with chain diamines, $NH_2(CH_2)_nNH_2$, have been the subject of several studies.[16,21,25] It was found that, for $n < 8$, 2D (or pseudo-

2D) topologies are favored with chain molecules oriented parallel to the inorganic layers. Starting from $n = 9$, the length of the aliphatic chain becomes a structure-driving force in the self-assembly of organic molecules that form either 1D micelles[21] or 2D blocks[25] (in both cases, hydrophobic fragments are hidden inside the micelle or block and amine head groups are located on the surface). It is important to note that the surface charge density of uranyl oxysalt layers is usually lower than that of the other oxysalts (e.g., transition metal phosphates, etc.), as a result of the large surface area occupied by equatorial base planes of uranyl bipyramids. The surface charge density of diamine blocks is two times higher than that of uranyl oxysalt layers. This discrepancy results in the inclusion of acid–water complexes into the organic blocks, which modifies its charge density in order to achieve structural stability.[25] In turn, 1D micelles with cross-like orientation of long diamine chains maintain their charge density without inclusion of additional components.

The influence of the shape and composition of organic templates upon the topology of uranyl selenate layers with a U/Se ratio of 2:3 has been studied.[16] As it was mentioned above, there are two different topologies based on $[(UO_2)_2(SeO_4)_3(H_2O)]^{2-}$ layers shown in Figure 2. Experimental studies of the formation of these topologies in the presence of different amines revealed that aliphatic components of amine molecules tend to associate with six-membered rings of the inorganic layers. As a result, molecules with longer and spacious aliphatic components favor formation of the layers with topology **2**, whereas those with shorter aliphatic components prefer layers with the topology **1**. Several particular examples of mutual orientation of chain diamine molecules with topology of the inorganic layer is shown in Figure 12.

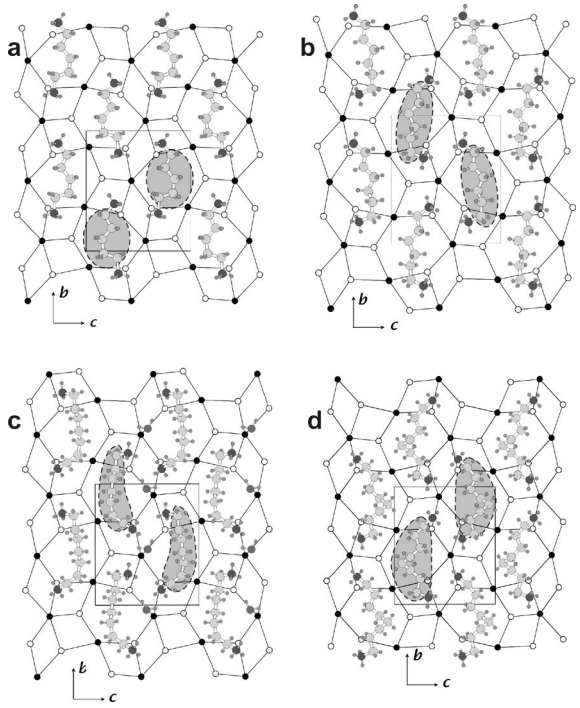

Figure 12. Location of the protonated amine molecules in the structures of $[C_5H_{16}N_2][(UO_2)_2(SeO_4)_3(H_2O)]$, $[(UO_2)_2(SeO_4)_3(H_2O)](H_2O)$, $[C_7H_{20}N_2][(UO_2)_2(SeO_4)_3(H_2O)](H_2O)$, and $[C_8H_{22}N_2][(UO_2)_2(SeO_4)_3(H_2O)]$ relative to the black-and-white graph of the inorganic layer (a, b, c, d, respectively).

6. Origin of Structural Diversity: An Exercise in Cellular Automata Modeling

6.1. Methylamine-Templated Uranyl Selenates: Ordered and Disordered Structures

Gurzhiy et al.[26] investigated phase formation in the system $UO_2(NO_3)_2/H_2SeO_4$/methylamine/H_2O and found at least eight different crystalline uranyl selenates with U/Se = 1:2, 2:3, 3:5, and 5:8, some of them metastable or unstable in air. Of particular interest is the family of structures with general formula $(CH_3NH_3)[(UO_2)(SeO_4)_2(H_2O)](H_2O)_n$, where $n = 0$, 0.5, 1. The structures are based upon complex units with composition $[(UO_2)(SeO_4)_2(H_2O)]^{2-}$, but with different topologies of linkage of U and Se polyhedra for different values of n. For $n = 1$, the structure contains 1D chains (Figure 13a), for $n = 0$ the structure is based upon 2D layers (Figure 13b). For $n = 0.5$, a disordered structure was observed that represents a superposition of the 1D and 2D structures (Figure 14). Transition between two overlapping configurations can be achieved by a 1/2 translation of the [1+4+1] unit (see above). It is important to note that all

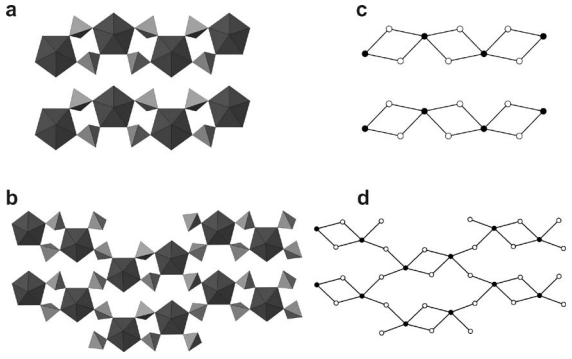

Figure 13. Uranyl selenate layers in the structures of $(CH_3NH_3)[(UO_2)(SeO_4)_2(H_2O)](H_2O)_n$, where $n = 0$ (a) and 1 (b) and their graphs [(c) and (d), respectively].

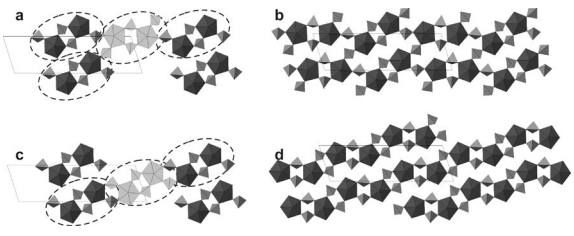

Figure 14. The uranyl selenate layer in the structure of $(CH_3NH_3)[(UO_2)(SeO_4)_2(H_2O)](H_2O)_{0.5}$ can be represented as a superposition of two different structures related to each other by translation of the [1+4+1] complex (highlighted) by 1/2 translation (a, c), which results in formation of either 2D (b) or 1D (d) ordered structures.

three structures shown in Figures 13 and 14 can be obtained by successive polymerization of the [1+4+1] cluster, which supports our suggestion concerning its existence as a prenucleation building block in aqueous solutions. Thus, in the $(CH_3NH_3)[(UO_2)(SeO_4)_2(H_2O)](H_2O)_n$ family, the appearance of disordered structure with $n = 0.5$ can be represented as an oscillation of the growth process between the structure types with $n = 0$ and 1. This process can be modeled by construction of abstract dynamic systems known as cellular automata.

6.2. Cellular Automata: Basic Concepts

Cellular automata (CA) have been introduced for simulation of self-reproductive biological systems[27] and have attracted considerable attention as a possible environment for modeling of a broad range of physical objects and processes,[28] in particular, of periodic growth of complex chemical structures.[29]

From the formal point of view, CA is defined as a collection of five basic components:
CA := $<Z, S, N, f, B>$,
where Z is a lattice (discrete working space of the CA consisting of cells; the simplest example is a 2D plane filled with square cells); $S = \{0, 1, 2, ...\}$ is a finite number of values that the cells may take [usually, these values are associated with colors, e.g. $S = (0, 1)$ characterizes a binary (2-color) CA]; $N = \{-k_1, -k_1 + 1, ..., -1, 0, 1, ..., k_2 - 1, k_2\}$ is a neighborhood of CA action for 1D CA; the value of cell x_0 at time $t = 1$ is determined by the values of k_1 and k_2 cells on the left and right sides at the time $t = 0$ [in the simplest case, the neighborhood is symmetric $k_1 = k_2 = 1$ and has a radius $k_0 = 1$, that is, it consists of three cells ($k = 3$): x_{-1}, x_0, x_1; the value of cell x_0 at time $t = 1$ is determined by the values x_{-1}, x_0, x_1 at time $t = 0$]; f is a local transition function that works for a certain neighborhood (usually written as a set of rules of the form 010→1); and B is a boundary condition.

The example of a CA is shown in Figure 15. According to the Wolfram classification,[28c] the CA has a number of 90. Its local transition function can be written as f = {111→0, 110→1, 101→0, 100→1, 011→1, 010→0, 001→1, 000→0}. Using one black cell as an initial condition, this CA results in the formation of a branching pattern known as the Serpinsky triangle. It is obvious that, for modeling of periodic structures (that may work as diffraction lattices), one needs a specific class of CA.

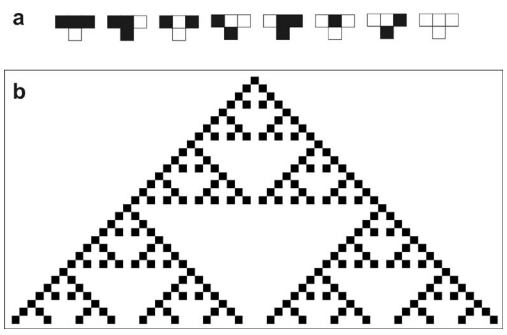

Figure 15. 1D cellular automaton 90: its transition rules (a) and the result of its work by the initial conditions given as a single black cell (b).

6.3. CA Model of Uranyl Selenate Structures and Their Growth

In order to construct CA that reproduce the formation of uranyl selenate structures with U/Se = 1:2, we topologically (i.e. without breaking of bonds) transform the graphs shown in Figure 13c and d into the graphs shown in Figure 16a and b, respectively. In turn, these graphs may be replaced by a 2D cellular structure, where black and white vertices are replaced by black and gray cells, respectively (white cells are reserved for "empty" space regions) (Figure 16c and d). The cells that share common edges correspond to the vertices linked by an edge. As a result, we have two tricolor cellular structures shown in Figure 16e and f. Analysis of these structures indicate that they can be successively constructed by using ternary CA with transition rules shown in Figure 17. By assignment of values of 0, 1, and 2 to white, gray, and black cells, respectively, the set of transition rules can be written down as f = {000→0, 001→1, 002→0, 010→2, 011→0, 012→2, 020→1, 021→1, 022→0, 100→1, 101→1, 102→1, 110→0, 111→0, 112→0, 120→1, 121→1, 122→0, 200→1, 201→1, 202→1, 210→0, 211→1, 212→0, 220→0, 221→0, 222→0}.

Most of these rules are excessive in our case; however, they are used for the reasons of generality. This CA can be used to obtain the cellular structures shown in Figure 16e and f. This means that *the same* CA generates *different* structural topologies. The resulting topology is therefore determined by the initial conditions, that is, by the structure of the first row. In the language of chemistry, this could suggest that the molecular-level growth mechanism of uranyl selenate layers is the same and the topology of the structure is controlled by the structure of the nucleus spontaneously formed in solution.

In order to investigate the dependence of the structure topology on the structure of initial conditions, a computer experiment was performed by means of the Mathematica 6.0 program package.[30] The structure of the input row was given as an infinite periodic sequence of numbers 0, 1, and 2. Some results of the modeling are shown in Figure 18. The chain topology (Figure 18a) can be produced by using the sequence [0121], whereas the layer topology (Figure 18b) is the result of an input of the sequence [01012121]. The cellular structure shown in Figure 18c and resulting from input [12] deserves special attention. It corresponds to the structural unit shown in Figure 19b (graph depicted in Figure 19a), which has the composition $[(AnO_2)(TO_4)_2(H_2O)]$ and is observed in a large number of actinyl oxysalts, including uranyl selenates.[7] It is of interest that this unit can also be produced by using the CA described above.

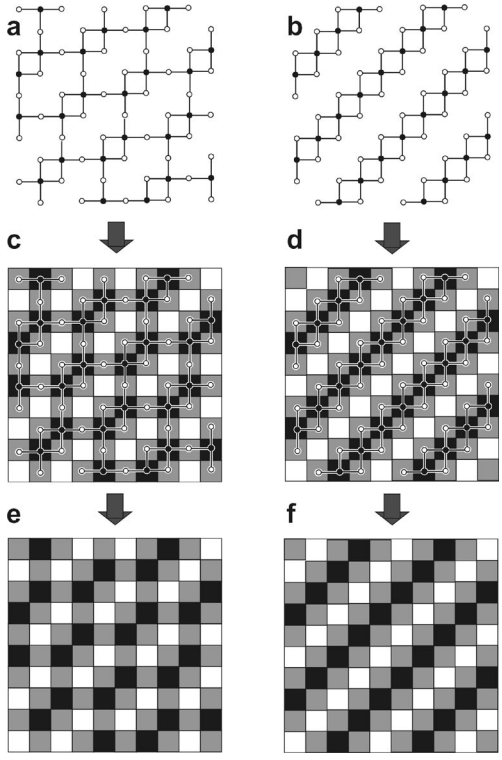

Figure 16. 2D (a) and 1D (b) graphs isomorphous to the graphs shown in Figure 13a and b, respectively, and their transformation to tricolor cellular structures (c–f).

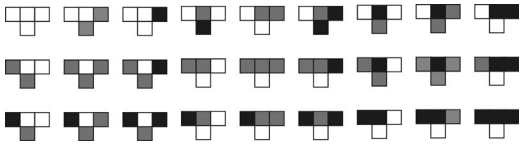

Figure 17. Visual representation of the local transition functions that can be used to generate the patterns shown in Figure 16e, f.

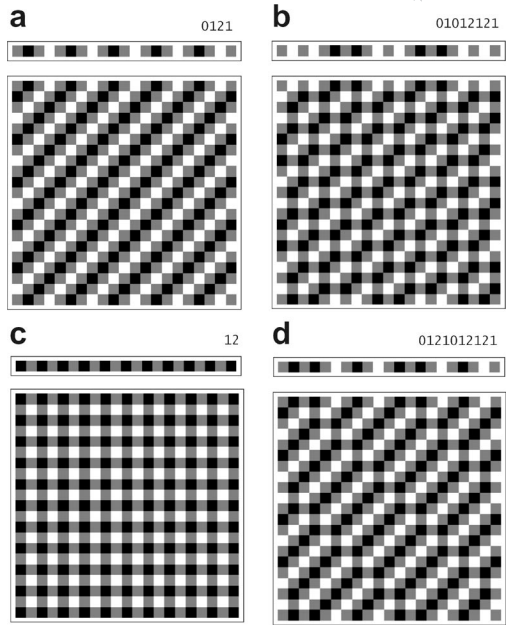

Figure 18. Examples of patterns generated by the automaton with the local transition function indicated in Figure 17 from initial conditions given as a periodic sequence of cells (periods are shown as numbers at the top right of each pattern). See text for details.

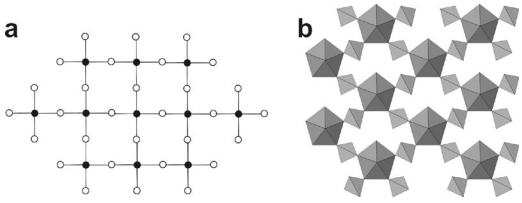

Figure 19. Black-and-white graph that corresponds to the cellular structure shown in Figure 18c (a) and the $[(AnO_2)(TO_4)_2(H_2O)]$ layer that has the same topology.

The results of computer modeling may shed some light into the process of self-assembly in uranyl selenate systems. In the case of ordered nuclei, either chain or layer topology is formed, whereas, in the case of disordered nuclei or growth faults (in computer language, errors of the CA function), a disordered topology is formed that represents a superposition of chain and layer topologies.

In general, rather simple examples of CA modeling of self-assembly processes in actinyl-based systems indicate that the theory of CA and finite automata may provide a coherent framework for the description of the dynamics of chemical systems, provided that an appropriate abstract model is constructed. Moreover, it seems feasible that, in the deep sense, growth of periodic structures is similar to the growth of cellular structures during the development of a CA, and crystal growth can therefore be viewed as a computation.

The parallels between chemical structures and such formal objects as CA can also be extended further. For instance, the CA theory contains the concept of a "Garden-of-Eden" configuration, which is a configuration that can never appear as a result of the specific CA work. In the case of a 1D automaton, this is the row of cells, which has no predecessors. There could be an infinite number of "Garden-of-Eden" configurations for a particular CA, and there are specific elementary configurations that any "Garden-of-Eden" contains. These configurations are called orphans. By inspection of the CA rules shown in Figure 17, it is easy to conclude that, for the given transition functions, sequences [11] and [22] are orphans, that is, they may not form as the result of the CA work under any circumstances. Translating these sequences into the language of chemistry, this could imply that, in our system, no uranyl dimers or diselenate groups Se_2O_7 may form. Indeed, formation of uranyl dimers is generally possible (with bridging hydroxy of fluoride ions), but not under acidic conditions employed in our particular experiment. Formation of diselenate groups is also rather impossible, taking into account their instability relative to the monoselenate groups.

Application of CA allows the prediction of possible topologies that may form in a specific system. It may also provide a computational basis for studying complexity and dy-

namics of topologically and chemically similar structures forming under similar physico-chemical conditions.

7. Conclusions

In this review, we tried to demonstrate that the structural diversity of actinyl oxysalts with TO_4 tetrahedral oxyanions (T = S, Se, Cr, Mo) is truly remarkable, owing to the flexibility of the An–O–T links, which results in a multitude of topological and geometrical variations. At least for a partial number of structures, this diversity may be understood and modeled by using abstract mathematical and computer science theories such as graph theory and cellular automata. Even more deep understanding is required in order to be able to engineer specific inorganic architectures and nanoscale structures in this family by the interplay between properties of organic templates and topological features of prenucleation secondary building units.

Acknowledgments

This work was supported by the President of Russian Federation Grant (No. MD-407.2009.5) and the Programme of Presidium of the Russian Academy of Sciences.

[1] R. J. Finch, T. Murakami, *Rev. Mineral.* **1999**, *38*, 91–179.
[2] E. C. Buck, D. J. Wronkiewicz, P. A. Finn, J. K. Bates, *J. Nucl. Mater.* **1997**, *249*, 70–76.
[3] N. L. Misra, K. L. Chawla, V. Venugopal, N. C. Jayadevan, D. D. Sood, *J. Nucl. Mater.* **1995**, *226*, 120–127.
[4] R. A. Penneman, R. G. Haire, M. H. Lloyd in *Actinide Separations, ACS Symp. Ser. 117* (Eds.: J. D. Navratil, W. W. Schulz), American Chemical Society, Washington, DC, **1980**, pp. 571–581.
[5] a) E. C. Buck, N. R. Brown, N. L. Dietz, *Environ. Sci. Technol.* **1996**, *30*, 81–88; b) Y. Roh, S. Y. Lee, M. P. Elles, K. S. Cho, *J. Env. Sci. Health* **2000**, *A35*, 1043–1059.
[6] a) D. J. Wronkiewicz, J. K. Bates, T. J. Gerding, E. Veleckis, B. S. Tani, *J. Nucl. Mater.* **1992**, *190*, 107–127; b) D. J. Wronkiewicz, J. K. Bates, S. F. Wolf, E. C. Buck, *J. Nucl. Mater.* **1996**, *238*, 78–95; c) R. J. Finch, E. C. Buck, P. A. Finn, J. K. Bates, *Mater. Res. Soc. Symp. Proc.* **1999**, *556*, 431–437; d) A. P. Deditius, S. Utsunomia, R. C. Ewing, *J. Alloys Compd.* **2007**, *444–445*, 584–589.
[7] S. V. Krivovichev, P. C. Burns in *Structural Chemistry of Inorganic Actinide Compounds* (Eds.: S. V. Krivovichev, P. C. Burns, I. G. Tananaev), Elsevier, Amsterdam, **2007**, pp. 95–182.
[8] a) E. E. Baeva, A. V. Virovets, E. V. Peresypkina, L. B. Serezhkina, *Russ. J. Inorg. Chem.* **2006**, *51*, 220–228; b) E. E. Baeva, A. V. Virovets, E. V. Peresypkina, L. B. Serezhkina, *Russ. J. Inorg. Chem.* **2006**, *51*, 210–219; c) T. Z. Forbes, V. Goss, M. Jain, P. C. Burns, *Inorg. Chem.* **2007**, *46*, 7163–7168; d) E. V. Alekseev, S. V. Krivovichev, W. Depmeier, T. Malcherek, E. V. Suleimanov, E. V. Chuprunov, *Z. Kristallogr.* **2007**, *222*, 391–395; e) E. V. Alekseev, S. V. Krivovichev, W. Depmeier, T. Malcherek, E. V. Suleimanov, E. V. Chuprunov, *Z. Anorg. Allg. Chem.* **2007**, *633*, 1979–1984; f) E. V. Alekseev, S. V. Krivovichev, T. Malcherek, W. Depmeier, *Inorg. Chem.* **2007**, *46*, 8442–8444; g) A. V. Marukhnov, V. N. Serezhkin, D. V. Pushkin, O. P. Smirnov, V. P. Plakhtii, *Russ. J. Inorg. Chem.* **2008**, *53*, 1283–1287; h) V. N. Serezhkin, I. V. Medrish, L. B. Serezhkina, *Russ. J. Coord. Chem.* **2008**, *34*, 146–155; i) R. E. Wilson, S. Skanthakumar, K. E. Knope, C. L. Cahill, L. Soderholm, *Inorg. Chem.* **2008**, *47*, 9321–9326; j) V. Vlček, J. Čejka, I. Císařová, V. Goliáš, J. Plášil, *J. Mol. Struct.* **2009**, *936*, 75–79; k) J. Ling, G. E. Sigmon, P. C. Burns, *J. Solid State Chem.* **2009**, *182*, 402–408; l) T. Z. Forbes, P. C. Burns, *J. Solid State Chem.* **2009**, *182*, 43–48.
[9] a) Yu. N. Mikhailov, L. A. Kokh, V. G. Kuznetsov, T. G. Grevtseva, S. K. Sokol, G. V. Ellert, *Koord. Khim.* **1977**, *3*, 508–513; b) L. A. Hayden, P. C. Burns, *J. Solid State Chem.* **2002**, *163*, 313–318; c) A. J. Norquist, M. B. Doran, D. O'Hare, *Inorg. Chem.* **2005**, *44*, 3837–3843; d) S. V. Krivovichev, *Radiochemistry* **2008**, *50*, 450–454; e) C. Hennig, A. Ikeda, K. Schmeide, V. Brendler, H. Moll, S. Tsushima, A. C. Scheinost, S. Skanthakumar, R. Wilson, L. Soderholm, K. Servaes, C. Görrler-Walrand, R. Van Deun, *Radiochim. Acta* **2008**, *96*, 607–611.
[10] a) S. V. Krivovichev, *Crystallogr. Rev.* **2004**, *10*, 185–232; b) S. V. Krivovichev, *Structural Crystallography of Inorganic Oxysalts*, Oxford University Press, Oxford, **2008**.
[11] a) N. A. Budantseva, G. B. Andreev, A. M. Fedoseev, M. Yu. Antipin, *Russ. J. Coord. Chem.* **2003**, *29*, 653–657; b) M. S. Grigor'ev, A. M. Fedoseev, N. A. Budantseva, A. A. Bessonov, J.-C. Krupa, *Crystallogr. Rep.* **2004**, *49*, 676–678; c) M. B. Doran, A. J. Norquist, C. L. Stuart, D. O'Hare, *Acta Crystallogr., Sect. E* **2004**, *60*, m996–m998; d) S. V. Krivovichev, V. Kahlenberg, *Z. Anorg. Allg. Chem.* **2005**, *631*, 739–744; e) S. V. Krivovichev, P. C. Burns, *Z. Kristallogr.* **2003**, *218*, 725–732; f) S. V. Krivovichev, V. Kahlenberg, *Z. Anorg. Allg. Chem.* **2004**, *630*, 2736–2742; g) M. S. Grigor'ev, A. M. Fedoseev, N. A. Budantseva, *Russ. J. Coord. Chem.* **2003**, *29*, 877–880.
[12] S. V. Krivovichev, P. C. Burns, *Z. Kristallogr.* **2003**, *218*, 568–574.
[13] V. N. Serezhkin, V. K. Trunov, *Kristallografiya* **1981**, *26*, 301–304.
[14] N. P. Brandenburg, B. O. Loopstra, *Cryst. Struct. Commun.* **1973**, *2*, 243–246.
[15] S. V. Krivovichev, P. C. Burns, *Z. Kristallogr.* **2003**, *218*, 683–690.
[16] S. V. Krivovichev, V. V. Gurzhiy, I. G. Tananaev, B. F. Myasoedov, *Dokl. Phys. Chem.* **2006**, *409*, 228–232; S. V. Krivovichev, V. V. Gurzhiy, I. G. Tananaev, B. F. Myasoedov, *Z. Kristallogr.* **2009**, *224*, 316–324.
[17] a) P. C. Burns, K.-A. Kubatko, G. Sigmon, B. J. Fryer, J. E. Gagnon, M. R. Antonio, L. Soderholm, *Angew. Chem. Int. Ed.* **2005**, *44*, 2135–2139; b) T. Z. Forbes, J. G. McAlpin, R. Murphy, P. C. Burns, *Angew. Chem. Int. Ed.* **2008**, *47*, 2824–2827; c) G. E. Sigmon, J. Ling, D. K. Unruh, L. Moore-Shay, M. Ward, B. Weaver, P. C. Burns, *J. Am. Chem. Soc.* **2009**, *131*, 16648–16649; d) G. E. Sigmon, D. K. Unruh, J. Ling, B. Weaver, M. Ward, L. Pressprich, A. Simonetti, P. C. Burns, *Angew. Chem. Int. Ed.* **2009**, *48*, 2737–2740.
[18] L. Soderholm, P. M. Almond, S. Skanthakumar, R. E. Wilson, P. C. Burns, *Angew. Chem. Int. Ed.* **2008**, *47*, 298–302.
[19] a) G. Nocton, F. Burdet, J. Pécaut, M. Mazzanti, *Angew. Chem. Int. Ed.* **2007**, *46*, 7574–7578; b) P. Thuéry, *Inorg. Chem. Commun.* **2008**, *11*, 616–620; c) P. Thuéry, *Cryst. Growth Des.* **2009**, *9*, 4592–4594.
[20] a) S. V. Krivovichev, V. Kahlenberg, R. Kaindl, E. Mersdorf, I. G. Tananaev, B. F. Myasoedov, *Angew. Chem. Int. Ed.* **2005**, *44*, 1134–1136; b) S. V. Krivovichev, V. Kahlenberg, I. G. Tananaev, R. Kaindl, E. Mersdorf, B. F. Myasoedov, *J. Am. Chem. Soc.* **2005**, *127*, 1072–1073; c) E. V. Alekseev, S. V. Krivovichev, W. Depmeier, *Angew. Chem. Int. Ed.* **2008**, *47*, 549–551.
[21] S. V. Krivovichev, V. Kahlenberg, R. Kaindl, E. Mersdorf, *Eur. J. Inorg. Chem.* **2005**, 1653–1656.
[22] a) Yu. N. Mikhailov, Yu. E. Gorbunova, E. A. Demchenko, L. B. Serezhkina, V. N. Serezhkin, *Zh. Neorg. Khim.* **2000**, *45*, 1711–1713; b) A. J. Norquist, P. M. Thomas, M. B. Doran, D. O'Hare, *Chem. Mater.* **2002**, *14*, 5179–5184; c) A. J. Norquist, M. B. Doran, P. M. Thomas, D. O'Hare, *Dalton Trans.* **2003**,

1168–1175; d) A. J. Norquist, M. B. Doran, P. M. Thomas, D. O'Hare, *Inorg. Chem.* **2003**, *42*, 5949–5953; e) A. J. Norquist, M. B. Doran, D. O'Hare, *Solid State Sci.* **2003**, *5*, 1149–1158; f) P. M. Thomas, A. J. Norquist, M. B. Doran, D. O'Hare, *J. Mater. Chem.* **2003**, *13*, 88–92.

[23] a) P. S. Halasyamani, R. J. Francis, S. M. Walker, D. O'Hare, *Inorg. Chem.* **1999**, *38*, 271–279; b) S. V. Krivovichev, P. C. Burns, *J. Solid State Chem.* **2003**, *170*, 106–117; c) S. V. Krivovichev, C. L. Cahill, E. V. Nazarchuk, P. C. Burns, T. Armbruster, W. Depmeier, *Microporous Mesoporous Mater.* **2005**, *78*, 209–215.

[24] a) S. V. Krivovichev, I. G. Tananaev, V. Kahlenberg, B. F. Myasoedov, *Radiochemistry* **2006**, *48*, 213–216; b) L. B. Serezhkina, E. V. Peresypkina, A. V. Virovets, A. G. Verevkin, D. V. Pushkin, *Crystallogr. Rep.* **2009**, *54*, 259–266.

[25] S. V. Krivovichev, I. G. Tananaev, B. F. Myasoedov, *C. R. Chim.* **2007**, *10*, 897–904.

[26] V. V. Gurzhiy, V. V. Kovrugin, S. V. Krivovichev, I. G. Tananaev, B. F. Myasoedov, *Radiochem.*, accepted.

[27] J. von Neumann, in *Celebral Mechanisms in Behaviour: The Hixon Symposium* (Ed.: L. A. Jeffress), Wiley, New York, **1951**, pp. 1–32.

[28] a) T. Toffoli, N. Margolus, *Cellular Automata Machines: A New Environment for Modeling*, MIT Press, Boston, **1987**; b) A. Ilachinski, *Cellular Automata: A Discrete Universe*, World Scientific, New Jersey, London, Singapore, Hong Kong, **2001**; c) S. Wolfram, *A New Kind of Science*, Wolfram Media, Inc., Urbana, **2002**.

[29] a) A. Mackay, *Phys. Bull.* **1976**, 495; b) S. Krivovichev, *Acta Crystallogr., Sect. A* **2004**, *60*, 257–262; c) V. Ya. Shevchenko, S. V. Krivovichev, *Struct. Chem.* **2008**, *19*, 571–577; d) V. Ya. Shevchenko, S. V. Krivovichev, A. L. Mackay. *Glass Phys. Chem.* **2010**, *36*, 1–9.

[30] *Mathematica*, Wolfram Inc., **2008**.

Received: February 10, 2010
Published Online: May 25, 2010

